

Density Functional Theory Study of Atomic Nitrogen on the Si(100)–(2 × 1) Surface

Yuniarto Widjaja

Department of Chemical Engineering, Stanford University, Stanford, California 94305

Annica Heyman[†]

Department of Electrical Engineering, Stanford University, Stanford, California 94305

Charles B. Musgrave*

Departments of Chemical Engineering and Materials Science and Engineering, Stanford University, Stanford, California 94305

Received: August 29, 2001

Atomic nitrogen on the Si(100)–(2 × 1) surface is investigated using B3LYP density functional theory to study the incorporation of nitrogen atom into the silicon surface during growth of nitride films on silicon. Several possible structures for nitrogen on the Si(100)–(2 × 1) surface are investigated, including N bridge-bonded into the Si–Si dimer, N bridge-bonded into the Si–Si back-bond, and N inserted by forming three bonds with three Si atoms. Furthermore, the energetics and reaction mechanisms leading to these structures are also calculated. We find that the structure with nitrogen atom bridge-bonded into the Si–Si dimer to be the most thermodynamically stable, with an adsorption energy of 105 kcal/mol and an insertion barrier of 29 kcal/mol. Insertion into the Si–Si back-bond, however has the lowest activation barrier of 11 kcal/mol, although its adsorption energy is 13 kcal/mol lower than insertion into the Si–Si dimer. The third configuration investigated with N forming three bonds with Si atoms has a relatively high activation barrier of 35 kcal/mol and an adsorption energy of 95 kcal/mol. In addition, the formation of this structure “consumes” three Si atoms. Hence, at high nitrogen pressure, this structure is expected to be less dominant than those with N inserted into the Si–Si bonds, which only consume two Si atoms.

Introduction

Silicon nitride films have become pervasive in the microelectronics industry. They are, for example being used as insulators, oxidation masks, diffusion barriers and gate dielectrics.^{1–5} Currently, silicon nitride films are typically grown by chemical vapor deposition of NH₃ or mixtures of silicon containing precursors and NH₃. However, because the desired product is Si₃N₄, adsorption of nitrogen atom on silicon is the most direct way to achieve silicon nitride. Several nitrogen sources exist. For instance, N₂, N[–], and N are all possible N sources.^{6,7} The reason these are not widely used today is either due to their low reactivity, for example N₂, or the difficulty and/or cost of producing them, for example N[–] and N.

Here, we investigate the atomistic mechanism of the reaction of atomic nitrogen with the Si(100)–(2 × 1) surface to determine how nitrogen incorporates into growing nitride films. The kinetic and thermodynamic details of this process are expected to be valuable in the optimization of the deposition process and also in developing a detailed understanding of the deposition chemistry, which may also lead to better control of Si₃N₄ film properties. This knowledge becomes more valuable as the desired film thickness required for integrated circuit devices decreases, for example in the use of silicon nitride in high- κ gate stacks. In addition, the results also provide insight

into how nitrogen from other nitrogen-containing precursors, such as NH₃ or N₂, incorporates into the silicon surface. For instance, in the nitridation of Si(100) by ammonia, NH₃ first dissociates to form NH₂(a) and H(a). These species are stable below 700 K above which NH₂(a) undergoes further decomposition to N(a),^{8–10} in which H₂ desorption is thought to be the rate-limiting step.^{11–13}

Despite its importance, to our knowledge, the reaction of atomic nitrogen on the Si(100)–(2 × 1) surface has not received much attention. The studies that have been performed were done at high temperatures, preventing the detailed mechanism at lower temperatures from being probed, and mostly are done on Si-(111).^{7,14,15} Here, we investigate the detailed chemical mechanism of the reaction of N with the Si(100)–(2 × 1) surface using density functional theory (DFT) calculations. We perform geometry optimizations and calculate the energies of the stationary points on the potential energy surface (PES), including stable species and transition states between these species. Recently, Ueno and Ornellas published DFT results on the quadruplet spin state of N atom on Si (100)–(2 × 1).¹⁶ In contrast, we obtain the ground-state energies for stationary points on the N atom on Si (100)–(2 × 1) potential energy surface, which are different from those of Ueno and Ornellas. However, even for systems with the same spin multiplicity, such as the adsorbed state, we find significant quantitative difference with their results. The N atom adsorption energy we obtain is different from that reported by Ueno and Ornellas because the position of the N atom relative to the surface in their reactant state is

* To whom correspondence should be addressed. E-mail: charles@chemeng.stanford.edu; Phone: (650) 725–9176.

[†] Present address: Department of Physics and Measurement Technology, IFM, Linköping University, Linköping, Sweden.

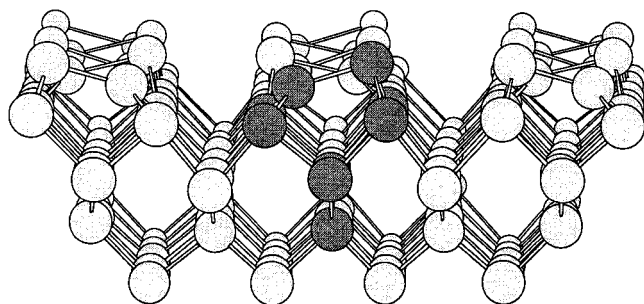


Figure 1. (2×1) reconstructed Si(100) surface and the one-dimer cluster, shown in black.

constrained resulting in an unfavorable interaction energy. On the other hand, our separated state involves no interaction. We have also predicted an additional stable structure, which we expect to be the dominant surface species. We will highlight comparisons between our results and those of Ueno and Ornellas in the Discussion section, including our attempts to reconcile the observed differences.

Computational Details

Our theoretical approach is based on DFT quantum chemical simulations of cluster models of the silicon surface and QCISD(T) (quadratic configuration-interaction singles and doubles excitations including the triples correction) calculations for calibration of the DFT energies. The (2×1) -reconstructed Si(100) surface is shown in Figure 1, which also shows the one-dimer cluster (Si_9H_{12}) used to model the surface in this study. The one-dimer cluster includes two surface Si atoms representing the dimer structure, four second layer Si atoms, two-third layer Si atoms, and one-fourth layer Si atom. Hydrogen atoms are used to terminate the dangling bonds resulting from the truncation of the bulk Si–Si bonds. These hydrogens serve to maintain the tetrahedral sp^3 bonding environment of the subsurface Si atoms. However, the electronegativity difference between silicon and hydrogen may create a chemical environment at the cluster boundary that is different from the actual Si(100)– (2×1) surface. Hydrogen is more electronegative than silicon and, therefore, will withdraw charge from the Si atoms. Redondo et al. have proposed using “pseudoatoms”, which are modified H atoms referred to as “siligens”, such that the siligens have the same electronegativity as bulk Si atoms.^{17–19} However, subsequent studies by Illas et al.²⁰ and by Pai and Doren²¹ have shown almost negligible effects of the siligen pseudoatoms and can possibly lead to errors in predicting bond energies. We have also used cluster models of various sizes to determine that the error caused by these terminating hydrogens is insignificant.²² The one-dimer cluster is also designed to mimic the strain of the surrounding material. This is accomplished by imposing geometric constraints, which are obtained through a two-step procedure as described previously.²² In addition to the one-dimer cluster, we also use the $\text{Si}_{12}\text{H}_{20}$ three-dimer cluster, which includes two neighboring dimers along the dimer row, to investigate the nonlocal electronic and strain effects exerted by neighboring silicon atoms.

We use the B3LYP three-parameter density functional theory (DFT) method with the Becke “hybrid” gradient-corrected exchange functional and the Lee–Yang–Parr correlation functional.^{23–25} The exchange functional is a linear combination of Dirac’s local, Becke’s 1988 nonlocal, and exact (Hartree–Fock) exchange terms. B3LYP has been shown to achieve significant accuracy at only a modest increase in cost over Hartree–Fock. Our recent comparisons of B3LYP and

QCISD(T)²⁶ on small cluster models demonstrate that B3LYP describes the reaction of NH_3 on Si(100)– (2×1) accurately.^{22,27} DFT has also been used to study other Si–N systems. For instance, Jungnickel et al. have calculated the structure and energetics of Si_nN_m clusters and their growth pathways using DFT.²⁸

The electronic wave function is expanded in a mixed Gaussian basis set. A diffuse triple- ζ plus polarization 6-311++G(2d,p) basis set is used to describe the chemically active atoms, i.e., the surface Si atoms, four Si atoms of the first subsurface layer, and the N atom. The remaining subsurface silicon atoms and terminating hydrogen atoms are described at the double- ζ plus polarization 6-31G(d) level. This mixed-basis set scheme accurately describes the orbitals directly involved in the reaction while limiting the computational expense of the simulations. All calculations are performed using the Gaussian 98 program.²⁹

Results

Nitrogen Atom. We calculate the two lowest spin states of N, doublet and quadruplet. The open-shell calculations are performed by using separate spatial orbitals for electrons with different spins. The ground state is found to be quadruplet, with the doublet state 67 kcal/mol higher in energy. This agrees with Hund’s rules, which state that the quadruplet state is the ground state because it maximizes the total spin of the atom because it has three unpaired electrons. The doublet-quadruplet splitting of 67 kcal/mol calculated using B3LYP is found to agree with the corresponding value calculated using QCISD(T) of 66 kcal/mol. The state with a spin multiplicity of 6 has also been calculated and the energy found to be 378 kcal/mol higher than the quadruplet state, further confirming the quadruplet state as the ground state.

Nitrogen Adsorption onto the Si(100)– (2×1) Surface.

As has been shown both theoretically and experimentally, the dimers of the Si(100)– (2×1) surface are asymmetric, with one Si atom of the dimer pushed up and the other down.^{30–35} The two dimer atoms will hereafter be referred to as the “up” and “down” dimer atoms. To determine the most energetically favorable position for atomic nitrogen on the silicon surface, it is therefore necessary to investigate N adsorbed on both the “up” and “down” Si atoms. However, the optimized structure of the adsorbed state N(a), shown in Figure 2a, indicates that the surface dimer is no longer tilted with N adsorbed on it, removing the inequivalency between the dimer atoms.

Different spin multiplicities (doublet and quadruplet) are also investigated. We find that the ground state has a spin multiplicity of 4 (quadruplet). However, the difference between the doublet and quadruplet states is less than 1 kcal/mol, in contrast to the large splitting between these spin states for atomic N. This result is expected because the remaining unpaired electron on the silicon dimer has little overlap with the two unpaired N electrons.

The adsorption energy of atomic nitrogen on the Si(100)– (2×1) surface is 60 kcal/mol. The Si–N bond length is 1.76 Å, indicating that the bond is covalent, in contrast to NH_3 , which forms a dative bond on Si(100)– (2×1) .²⁷ This implies that the Si–N bond is formed between a nitrogen unpaired electron and one of the Si dangling bonds of the dimer. On the other hand, the Si–N bond formed in the adsorption of NH_3 results from the interaction between the NH_3 lone pair and the “empty-bond state” of the surface Si atom. As a result, the long-range order effects observed for NH_3 adsorption caused by donation of NH_3 lone pair electrons to the silicon surface is absent in

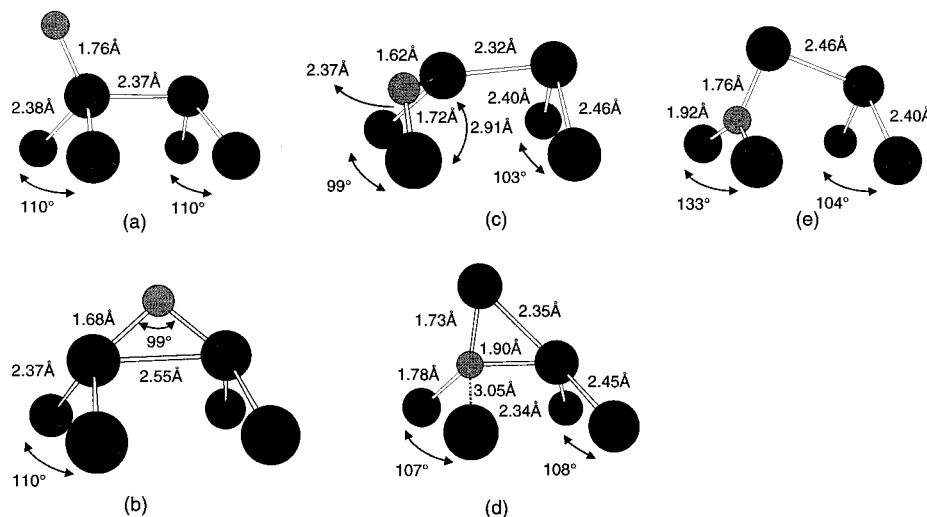


Figure 2. Structures of the stable configurations: (a) Adsorbed state, N(a); (b) N inserted into the Si-Si dimer, N(b); (c) N inserted into the Si-Si back-bond, N(2b); (d) Intermediate structure, N(3b-int); (e) N bonded to three Si atoms, N(3b)

TABLE 1: Enthalpies of Reaction and Activation Barriers of the Formation of the Stable Structures

structures	enthalpy of reaction (ΔH) in kcal/mol	transition state energy in kcal/mol
adsorbed state, N(a)	-60	
N inserted into the Si-Si dimer, N(b)	-105	-31 (29) ^a
N inserted into the Si-Si back-bond, N(2b)	-92	-49 (11) ^a
Intermediate structure leading to insertion of N into the subsurface, N(3b-int)	-89	-57 (35) ^b
N inserted into the subsurface layer, N(3b)	-95	-83 (6) ^c

Energies are relative to the sum of the clean Si(100)-(2 × 1) surface and atomic N energies, except transition state energies in parentheses which are with respect to the reference state noted in the footnotes. ^a This TS energy (in parenthesis) is given with respect to N(a). ^b This TS energy (in parenthesis) is given with respect to N(2b). ^c This TS energy (in parentheses) is given with respect to N(3b-int).

the case of atomic nitrogen adsorption, and consequently, the one-dimer cluster should be an appropriate model of the surface. Experimental results also support that no long-range effects exist.⁶ The adsorbed state geometry also shows an important distinction with the NH₃ adsorbed state. The Si surface dimer becomes flat upon adsorption of atomic nitrogen unlike the case of ammonia, which causes the dimer to become even more asymmetric.

We have also calculated the nitrogen adsorption energy using the Si₂₁H₂₀ three-dimer cluster, in which we obtained an adsorption energy of 59 kcal/mol, compared to the adsorption energy of 60 kcal/mol calculated with the one-dimer cluster. This further strengthens our arguments that long-range electronic effects are insignificant in this system and that the one-dimer cluster is an appropriate model.

Once nitrogen adsorbs onto the silicon surface, it can then undergo a number of different reactions. We investigate three different surface structures for N on the Si(100)-2 × 1 surface and the reaction mechanisms that lead to these configurations: N bridge-bonded into the Si-Si dimer, N bridge-bonded into the Si-Si back-bond, and N inserted by forming three bonds with three Si atoms. Hereafter, these configurations will be referred as N(b), N(bb), and N(3b), respectively. These structures are shown in Figure 2 and the energies and activation barriers of their formation are shown in Table 1.

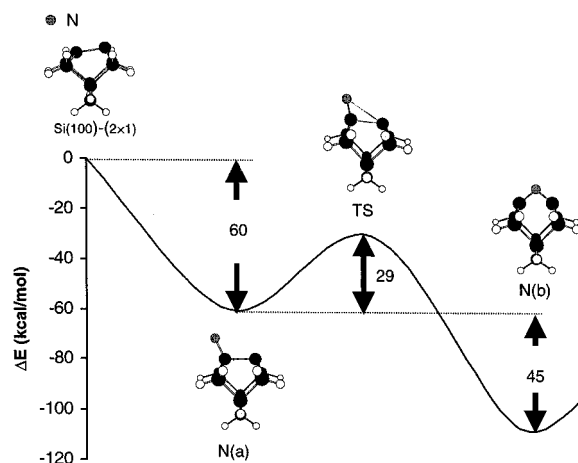


Figure 3. Reaction path and predicted energetics for insertion of N into the Si-Si dimer N(b).

Nitrogen Bridge-Bonded into the Si-Si Dimer. The reaction pathway and the reaction energetics of nitrogen insertion into the Si-Si dimer, N(b), are shown in Figure 3. The activation barrier for the reaction is 29 kcal/mol relative to the adsorbed state and the reaction is exothermic by 45 kcal/mol. The stability of this structure relative to the adsorbed state is due to the extra Si-N bond formed, which more than compensates for the ring strain energy of the three-membered ring. The optimized N(b) structure, as shown in Figure 2b, has *C*_{2v} symmetry and a Si-N bond length of 1.68 Å. This is shorter than the typical Si-N covalent bond length of 1.75 Å, which results from the strain of the three-member ring configuration.

The ground state of the bridge-bonded structure is doublet because two of the nitrogen atom electrons form covalent bonds with the two dangling bonds of the two dimer atoms. Thus, this leaves only one electron on the nitrogen atom unpaired, resulting in a spin multiplicity of 2. In addition, because both dangling bonds on the surface react with the N atom to form two covalent bonds, this configuration will result in a saturation coverage of one-half of a monolayer, with one nitrogen atom for every two silicon atoms.

Nitrogen Bridge-Bonded into the Si-Si Back-Bond. The potential energy surface (PES) for the N insertion into the Si-Si back-bond, N(2b), is shown in Figure 4. The activation energy for this insertion is 11 kcal/mol, lower than the corresponding insertion barrier into the Si-Si dimer of 29 kcal/mol. The

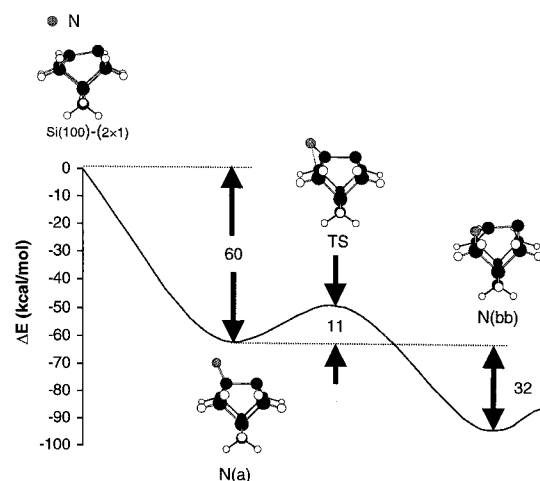


Figure 4. Reaction path and predicted energetics for insertion of N into the Si-Si back-bond N(2b).

reaction is however less exothermic compared to the insertion into the Si-Si dimer. The enthalpy of insertion into the Si-Si back-bond is 32 kcal/mol.

The reason this insertion is less exothermic than insertion into the Si-Si dimer can be seen from the geometry of the N(2b) structure, shown in Figure 2c. The Si-Si bond in which the insertion occurs is now stretched from 2.38 to 2.91 Å, further increasing the strain originating from the two surface silicons moving from their lattice positions to form the dimer reconstruction. We have calculated the strain associated with the dimer formation by performing calculations on an adamantane-like $\text{Si}_{10}\text{H}_{14}$ cluster model. This cluster models an isolated silicon surface atom of the unrelaxed surface prior to the dimer reconstruction. No neighboring surface atoms are present to prevent Si-Si dimer bond formation. The cluster also consists of two second layer, four-third layer, two-fourth layer, and one-fifth layer silicon atom and hydrogens to terminate the subsurface silicon atoms. All silicons are placed in tetrahedral, bulklike positions. The surface atom, which has two dangling bonds, is then moved to one of the surface positions, either the up or the down dimer position obtained from the one-dimer geometry. Because the surface silicon atom is isolated, the energy required to move the surface silicon atom is the local strain of the up or down dimer atom. The magnitude of this strain is found to be approximately 4 kcal/mol. Because insertion into the Si-Si dimer partially relieves this strain by pushing the dimers toward their original lattice positions and insertion into the Si-Si back-bond increases the strain by making the atoms of the dimer even more asymmetric, insertion into the dimer is more stable than insertion into the back-bond.

The N(2b) structure, shown in Figure 2c, reveals the nature of the N(2b) state asymmetry. The Si-N bond formed with the surface Si atom is 1.62 Å, whereas the Si-N bond formed with the subsurface Si is 1.72 Å. In addition, the dimer Si atom attached to the nitrogen now shifts "down". As previously discussed, the down dimer atom is electron deficient. Because of its lone pair electrons, nitrogen has a "negative" polarity, resulting in a stronger attraction between the "down" surface Si and the nitrogen atom, as opposed to the interaction between the "up" dimer atom and the nitrogen atom. This is confirmed by the Mulliken population analysis, which shows that the up Si atom is 0.85 e more positively charged than the down Si atom. Consequently, the bond between the N atom and the surface dimer atom is shorter than the corresponding bond

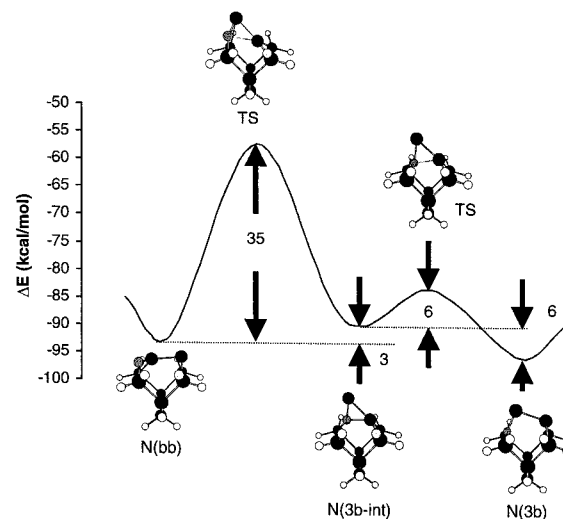


Figure 5. Reaction path and predicted energetics for insertion into the subsurface N(3b).

between the N atom and the subsurface Si. Hence, it can be seen that the two bridge-bonded structures (the insertion into the Si-Si dimer and the insertion into the Si-Si back-bond) have important distinctions leading to the differences in their stabilities.

Nitrogen Bonded to three Si Atoms. Another stable structure studied is the one with N bonded to three Si atoms; one surface Si atom and two subsurface Si atoms from the first surface sublayer. The atomistic mechanism to form this structure is shown in Figure 5. The starting structure is the one discussed previously, with N inserted into the Si-Si back-bond. As can be seen from the PES, the formation involves an intermediate structure, N(3b-int), shown in Figure 2d, in which N is bonded to two surface Si atoms and one subsurface Si atom. The activation barrier leading to the formation of this intermediate is calculated to be 35 kcal/mol relative to the energy of the N(2b) structure. The reaction is also endothermic with a reaction enthalpy of 3 kcal/mol.

From this intermediate, the N(3b) structure with N bonded to one surface Si atom and two subsurface Si atoms is then formed. This reaction has an activation barrier of 6 kcal/mol and the reaction is exothermic by 6 kcal/mol, both with respect to the energy of the intermediate N(3b-int). Because this activation barrier is lower than that of the N(3b-int) formation, the overall barrier for formation of the N(3b) structure is the barrier leading to the N(3b-int) intermediate of 35 kcal/mol.

The N(3b) configuration has an additional Si-N bond compared to the bridge bonded configurations. However, despite the extra Si-N bond, this configuration is only 3 kcal/mol more stable than the N(2b) structure. This is because in this configuration, shown in Figure 2e, although there are more Si-N bonds, the N-Si₃ structure is nearly planar. As a result, the N atom now has three sp^2 orbitals and one p orbital rather than four sp^3 orbitals that correspond to the tetrahedral configuration. The Si-N bonds for this configuration are 1.92 Å compared to 1.76 Å observed for "normal" unconstrained Si-N covalent bonds. The longer Si-N bonds indicate that they are weaker and the state is less stable. The position of the up dimer atom also indicates that this structure is very strained.

Comparing the N(3b) structure with the bridge-bonded N(b) structure, it can be seen that the insertion into the Si-Si dimer bond is more stable for the same reason. The planar N-Si₃ structure results in weaker Si-N bonds.

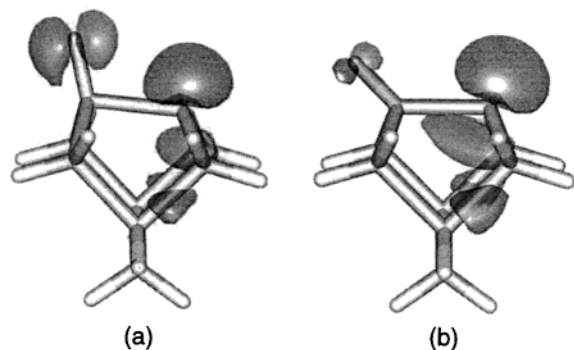


Figure 6. Molecular orbital of the transition state involved in the (a) insertion into the Si-Si dimer. The energy of this orbital is one orbital below the energy of the highest occupied molecular orbital (HOMO); (b) insertion into the Si-Si back-bond. This orbital is the highest occupied molecular orbital (HOMO) of this transition state.

Discussion

Comparing the energies of the three stable structures, we find that N inserted into the Si-Si dimer structure is the most favorable. The activation energy leading to the structure with atomic nitrogen inserted into the Si-Si back-bond is however 18 kcal/mol lower than the barrier to insert into the Si-Si dimer, although the product enthalpy is higher by 13 kcal/mol. The reason for this can be explained by an analysis of the molecular orbital of the transition states for both insertions, shown in Figure 6. Insertion of N atom into the Si-Si dimer requires changing the orientation of the unpaired electron orbital of the reacting Si dimer, which originally points away from the Si-Si dimer, so that good overlap with the N unpaired electron orbital can be formed. In contrast, insertion into the Si-Si back-bond does not require reorientation of the second layer Si orbitals. The new Si-N bond formed lies approximately in the direction of the broken Si-Si bond. As a result, the overlap between the N and Si orbitals is high. Consequently, the transition state energy for the insertion into the Si-Si back-bond is lower.

The N(3b) configuration with N bonded with two subsurface Si atoms and one surface Si atom, is more stable than the N(2b) structure, N inserted into the Si-Si back-bond. However, this structure consumes three Si atoms for one N atom. Therefore, at high N pressure, this configuration is expected to be less dominant. At high pressure, insertions into both the Si-Si dimer and Si-Si back-bond are expected to be dominant, as they only consume two Si atoms per nitrogen atom.

Schrott et al. have investigated the reaction of atomic nitrogen with the Si(100)-(2 × 1) surface using techniques such as thermal desorption, Auger spectroscopy, and electron energy loss spectroscopy (EELS).⁶ Their results indicate that the structure of the first reacted layer is relatively thick, although they did not report any quantitative results. The relatively thick first layer can be explained by examining the PES for all of the pathways considered here. The insertion barriers for all of the reactions we investigate are still below the energy of the initial reactants, i.e., atomic N and the clean surface, due to the exothermicity of the adsorption reaction. The question is whether the energy gained from the adsorption of nitrogen atom is available for subsequent reactions or not. If the energy transfer to the surface is inefficient, the adsorbing nitrogen will retain enough energy to overcome the barrier for the insertion reactions. As a result, this allows further reactions of N with the Si atoms of the surface and subsurface, which in turn yields thicker nitride films.

If the energy gained from the adsorption of nitrogen atom is efficiently transferred to the Si surface and the reactions proceed in the kinetically controlled regime, the N(2b) species will be prevalent on the surface. This is because the N(2b) formation activation barrier of 11 kcal/mol is the lowest among the pathways considered. High-resolution photoemission experiments by Peden et al. point to the existence of a monolayer of silicon at the outermost surface layer on top of the growing Si₃N₄ films.⁹ The N(2b) and N(3b) structures, in which nitrogen resides between the surface Si layer and the second Si layer, are possible structures which explain the above experimental results. However, as mentioned above, we predict formation of N(2b) to be favored over N(3b) at high pressures. This appears to be consistent with our proposed reaction mechanisms, which show that the N(2b) formation has the lowest activation barrier.

During the review of this paper, an article by Ueno and Ornellas that also investigates the adsorption of atomic N on Si(100)-(2 × 1) was published.¹⁶ The authors also employ the B3LYP method and use the cluster approach to model the silicon surface. The major difference in our approaches is that their investigation focuses solely on the quadruplet spin state PES, whereas we obtain the ground state of every stationary point investigated here. We find that except for the N(a) adsorbed state, which is a quadruplet, the remaining ground states are doublets.

Overall, our results show good qualitative agreement with Ueno and Ornellas's results. Their PES also shows the existence of the N(a) adsorbed state, the N(b) bridge-bonded state, and the N(3b) state. However, we predict a stable state where N has been inserted into a Si-Si back-bond (the N(2b) species), which is likely the dominant state because it is favored at high pressures, as discussed above. As also discussed above, the N(2b) species explains the results of the photoemission experiments relatively well.

However, despite the similar approaches, we find that there are significant quantitative differences in our results. For instance, we find an adsorption energy, which is the difference between the sum of the atomic nitrogen and the one-dimer cluster energies and the N(a) adsorbed state energy, of 60 kcal/mol. However, Ueno and Ornellas report an adsorption energy of 75 kcal/mol despite the use of the same method, cluster and spin multiplicity. The source of this discrepancy very likely originates from the unfavorable interaction between the N and the silicon surface in the reactant structure investigated by Ueno and Ornellas. Their reactant structure corresponds to an N atom symmetrically positioned 2.5 Å above the one-dimer cluster.³⁶ The constraint of having the nitrogen located symmetrically above the one-dimer cluster increases the energy relative to both the separated and product states and hence increases the adsorption energy.

Conclusion

We have investigated the reaction of atomic nitrogen on the Si(100)-(2 × 1) surface. We first examined the adsorption of N on the Si(100)-(2 × 1) surface. The Si-N bond formed in the adsorbed state is a covalent bond, in contrast to the dative bond formed in the adsorption of other nitrogen-containing species, such as ammonia or methylamines. The structure of the adsorbed state also shows a significant difference, in which the adsorption of atomic N yields an untilted Si dimer while adsorption of NH₃ makes the surface dimers more tilted. We then investigated three different stable structures that result from further reactions following the adsorbed state, i.e., N bridge-bonded into the Si-Si dimer N(b) structure, N bridge-bonded

into the Si–Si back-bond N(2b) structure, and N bonded with three Si atoms N(3b) structure. The reaction mechanisms leading to the formation of these structures are also investigated. The N(b) structure, which is N bridge-bonded into the Si–Si dimer, is the most stable structure thermodynamically, with an enthalpy of 105 kcal/mol below the sum of the atomic nitrogen and clean surface energies. The activation barrier for this insertion reaction is calculated to be 29 kcal/mol.

Insertions into the Si subsurface layers are found to be less stable than insertion into the Si–Si dimer. The enthalpy of reaction leading to the formation of the N(2b) structure is 92 kcal/mol below the sum of the atomic nitrogen and clean surface energies, whereas the enthalpy of reaction for the N(3b) structure is 95 kcal/mol. However, the insertion into the Si–Si back-bond has the lowest activation energy of 11 kcal/mol among the three pathways investigated. Nevertheless, because the activation energies for all reaction pathways lie below the energy of the initial reactants, we expect all of the three stable structures be formed, leading to a saturation coverage of more than a monolayer, and thus a slightly thicker initial nitride layer.

Acknowledgment. The authors thank Jason Weaver for insightful discussions. We would like to thank Joseph Han, Jeung Ku Kang, Collin Mui, Juan Senosiain, and Chuck Steinmetz for their help. Support of this work by the Powell Foundation, IBM, Hewlett-Packard, and LSI Logic are gratefully acknowledged. The research is also supported through computing resources provided by National Center for Supercomputing Applications (NCSA).

References and Notes

- (1) Hashimoto, A.; Kobayashi, M.; Kamijoh, T.; Takano, H.; Sakuta, M. *J. Electrochem. Soc.* **1986**, *133*, 1464.
- (2) Kooi, E.; Vanlierop, J. G.; Appels, J. A. *J. Electrochem. Soc.* **1976**, *123*, 1117.
- (3) *Silicon Nitride in Electronics*; Belyi, V. I., et al., Ed.; Elsevier: New York, 1988; Vol. 34.
- (4) Osenbach, J. W. *J. Appl. Phys.* **1988**, *63*, 4494.
- (5) Ma, Y.; Yasuda, T.; Lucovsky, G. *J. Vac. Sci. Technol. B* **1993**, *11*, 1533.
- (6) Schrott, A. G.; Su, Q. X.; Fain, S. C. *Surf. Sci.* **1982**, *123*, 223.
- (7) Schrott, A. G.; Fain, S. C. *Surf. Sci.* **1981**, *111*, 39.
- (8) Larsson, C. U. S.; Andersson, C. B. M.; Prince, N. P.; Flodstrom, A. S. *Surf. Sci.* **1992**, *271*, 349.
- (9) Peden, C. H. F.; Rogers, J. W.; Shinn, N. D.; Kidd, K. B.; Tsang, K. L. *Phys. Rev. B* **1993**, *47*, 15 622.
- (10) Taylor, P. A.; Wallace, R. M.; Choyke, W. J.; Dresser, M. J.; Yates, J. T. *Surf. Sci.* **1989**, *215*, L286.
- (11) Bater, C.; Sanders, M.; Craig, J. H. *Surf. Interface Anal.* **2000**, *29*, 208.
- (12) Bozso, F.; Avouris, P. *Phys. Rev. B* **1988**, *38*, 3937.
- (13) Widjaja, Y.; Musgrave, C. B. *Phys. Rev. B* **2001**, *64*, 205 303.
- (14) Schrott, A. G.; Fain, S. C. *Surf. Sci.* **1982**, *123*, 204.
- (15) Delord, J. F.; Schrott, A. G.; Fain, S. C. *J. Vac. Sci. Technol.* **1980**, *17*, 517.
- (16) Ueno, L. T.; Ornellas, F. R. *Surf. Sci.* **2001**, *490*, L637.
- (17) Redondo, A.; Goddard, W. A.; Swarts, C. A.; McGill, T. C. *J. Vac. Sci. Technol.* **1981**, *19*, 498.
- (18) Redondo, A.; Goddard, W. A.; McGill, T. C. *J. Vac. Sci. Technol.* **1982**, *21*, 649.
- (19) Redondo, A.; Goddard, W. A.; McGill, T. C. *Surf. Sci.* **1983**, *132*, 49.
- (20) Illas, F.; Roset, L.; Ricart, J. M.; Rubio, J. *J. Comput. Chem.* **1993**, *14*, 1534.
- (21) Pai, S.; Doren, D. *J. Phys. Chem.* **1994**, *98*, 4422.
- (22) Widjaja, Y.; Musgrave, C. B. *Surf. Sci.* **2000**, *469*, 9.
- (23) Becke, A. D. *J. Chem. Phys.* **1993**, *98*, 1372.
- (24) Becke, A. D. *Phys. Rev. A* **1988**, *38*, 3098.
- (25) Lee, C. T.; Yang, W. T.; Parr, R. G. *Phys. Rev. B* **1988**, *37*, 785.
- (26) Pople, J. A.; Head-Gordon, M.; Raghavachari, K. *J. Chem. Phys.* **1987**, *87*, 5968.
- (27) Widjaja, Y.; Mysinger, M. M.; Musgrave, C. B. *J. Phys. Chem. B* **2000**, *104*, 2527.
- (28) Jungnickel, G.; Frauenheim, T.; Jackson, K. A. *J. Chem. Phys.* **2000**, *112*, 1295.
- (29) Frisch, M. J.; Trucks, G. W.; Schlegel, H. B.; Scuseria, G. E.; Robb, M. A.; Cheeseman, J. R.; Zakrzewski, V. G.; Montgomery, J. A., Jr.; Stratmann, R. E.; Burant, J. C.; Dapprich, S.; Millam, J. M.; Daniels, A. D.; Kudin, K. N.; Strain, M. C.; Farkas, O.; Tomasi, J.; Barone, V.; Cossi, M.; Cammi, R.; Mennucci, B.; Pomelli, C.; Adamo, C.; Clifford, S.; Ochterski, J.; Petersson, G. A.; Ayala, P. Y.; Cui, Q.; Morokuma, K.; Malick, D. K.; Rabuck, A. D.; Raghavachari, K.; Foresman, J. B.; Cioslowski, J.; Ortiz, J. V.; Stefanov, B. B.; Liu, G.; Liashenko, A.; Piskorz, P.; Komaromi, I.; Gomperts, R.; Martin, R. L.; Fox, D. J.; Keith, T.; Al-Laham, M. A.; Peng, C. Y.; Nanayakkara, A.; Gonzalez, C.; Challacombe, M.; Gill, P. M. W.; Johnson, B. G.; Chen, W.; Wong, M. W.; Andres, J. L.; Head-Gordon, M.; Replogle, E. S.; Pople, J. A. *Gaussian 98*, revision A.5; Gaussian, Inc.: Pittsburgh, PA, 1998.
- (30) Over, H.; Wasserfall, J.; Ranke, W.; Ambiatello, C.; Sawitzki, R.; Wolf, D.; Moritz, W. *Phys. Rev. B* **1997**, *55*, 4731.
- (31) Wolkow, R. A. *Phys. Rev. Lett.* **1992**, *68*, 2636.
- (32) Munz, A. W.; Ziegler, C.; Gopel, W. *Phys. Rev. Lett.* **1995**, *74*, 2244.
- (33) Bullock, E. L.; Gunnella, R.; Patthey, L.; Abukawa, T.; Kono, S.; Natoli, C. R.; Johansson, L. S. O. *Phys. Rev. Lett.* **1995**, *74*, 2756.
- (34) Ramstad, A.; Brocks, G.; Kelly, P. J. *Phys. Rev. B* **1995**, *51*, 14 504.
- (35) Landemark, E.; Karlsson, C. J.; Chao, Y. C.; Uhrberg, R. I. G. *Phys. Rev. Lett.* **1992**, *69*, 1588.
- (36) Ueno, L. T.; Ornellas, F. R., *personal communication*, 2001.